Fusion Engineering and Design 8 (1989) 305–310
North-Holland, Amsterdam

MATERIAL SELECTION FOR THE TITAN REVERSED-FIELD PINCH REACTOR

S. SHARAFAT *, N.M. GHONIEM *, P.I.H. COOKE *,** and The TITAN Research Group

Department of Mechanical, Aerospace and Nuclear Engineering, and Institute for Plasma and Fusion Research, University of California, Los Angeles, Los Angeles, CA 90024-1597, USA

The operating conditions of a compact, high neutron wall loading fusion reactor severely limit the choices for structural, shield, insulator and breeder materials. In particular, the response of plasma-facing materials to radiation, thermal and pressure stresses, and their compatibility with coolants are of primary concern. Material selection issues were investigated for the compact, high mass power density TITAN reactor design study. In this paper the major findings regarding material performance are summarized. The retention of mechanical strength at relatively high temperatures, low thermal stresses, and compatibility with liquid lithium make vanadium-based alloys a promising material for structural components. The thermal creep behavior of V–3Ti–1Si and V–15Cr–5Ti alloys has been approximated. In addition, irradiation behavior including the effects of helium generation and coolant compatibility issues were investigated which led to the choice of V–3Ti–1Si as the primary structural material candidate for the liquid-lithium-cooled TITAN-I. For the water-cooled TITAN-II reactor, ferritic alloys are favored among structural material candidates. Depending on the choice of lithium salt dissolved in water, the radiolytic effects and corrosion characteristics of the aqueous breeding solution may be severe. LiOH and $LiNO_3$ have been identified as the most viable salts; however, the radiolytic and corrosion behavior of these salts in aqueous solutions differ substantially. The radiolytic behavior of the aqueous salt solutions has been examined and various molecular decomposition product yields were estimated for the TITAN-II irradiation conditions. Insulator material issues of concern include irradiation induced swelling and radiation-induced conductivity. Both issues have been investigated and operating temperatures for minimum swelling and dielectric breakdown strength have been identified for spinel ($MgO–Al_2O_3$). The high heat flux and sputtering/erosion issues limit the choice of the materials for the divertor target plate. Mechanical properties of various tungsten–rhenium alloys have been investigated. A highly ductile W–Re alloy containing 26 atomic percent rhenium was identified as a viable plasma-facing material.

1. Introduction

Two different safety issues play a role in the economic feasibility of fusion power. One is the level of demonstrable public safety and the other is the capital investment safety. From a public point of view minimizing radioactive inventory and designing an inherently and passively safe reactor are desired. Both of these issues are a direct function of the material choices made. Capital investment risks can be minimized if structural materials are selected to withstand accidents of highest severity without inflicting major damage to the fusion power core (FPC).

The TITAN reactor study was undertaken to study the aspects of economic and engineering feasibility and safety of a compact fusion reactor. TITAN [1] is a compact, high-power-density reactor (major radius 3.9 m, plasma minor radius 0.6 m, neutron wall loading 18 MW/m^2), based on the reversed-field-pinch (RFP) confinement concept. Two options for the TITAN fusion power core were considered: TITAN-I, a liquid-lithium-cooled design with a vanadium-based alloy structure, and TITAN-II, an aqueous lithium-salt-solution-cooled design with a low activation, high strength ferritic alloy as structure. Summaries of the TITAN-I and TITAN-II reactor designs can be found in refs. [2] and [3].

Many of the engineering feasibility and safety-related issues of such a fusion reactor hinge on material performances under normal and off-normal operating conditions. The material selection effort concentrates on fulfilling these performance and safety requirements. The TITAN-I and TITAN-II material selection issues are summarized in this paper. A more detailed discussion of the material selection efforts can be found in ref. [4].

* University of California, Los Angeles.
** Permanent address: UKAEA Culham Lab., Abingdon, Oxon OX14 3DB, U.K.

0920-3796/89/$03.50

2. TITAN-I structural materials

TITAN-I is a self-cooled liquid lithium design. The retention of mechanical strength at relatively high temperatures, low thermal stresses, and compatibility with liquid lithium make vanadium-based alloys a promising material for structural components. Compared with HT-9, vanadium-based alloys have better physical properties such as higher melting temperature, lower thermal expansion coefficient and lower density. The high melting temperature ($T_m = 1890\,^\circ C$) can have a significant bearing on safety-related issues. The higher ultimate tensile strength ($\sigma_u \sim 600$ MPa at 600 °C), lower expansion coefficient and slightly higher thermal conductivity of vanadium-based alloys results in higher heat load capabilities. When compared with ferritic alloys at a nominal neutron wall loading of 1 MW/m^2, vanadium-based alloys have about half the nuclear heating rate (~ 25 W/cm^3), about a third of the helium generation rate (~ 57 He-appm), about half the hydrogen production rate (~ 240 H-appm/MW-yr/m^2) and lower long-term after-heat [5].

Among the various vanadium-based alloys the most promising candidates for fusion reactor applications are V–15Cr–5Ti, VANSTAR-7(V–9Cr–3Fe–1Zr), and V–3Ti–1Si. In the past, the V–15Cr–5Ti alloy had been adopted as the class model alloy in the U.S. In particular, V–15Cr–5Ti has a higher thermal creep resistance than the other two alloys. Investigation of the effects of neutron irradiation with pre-implanted helium atoms, however, suggest that V–15Cr–5Ti may be subject to unacceptable losses in ductility [6]. Braski [6] irradiated specimens of V–15Cr–5Ti, V–3Ti–1Si and VANSTAR-7 at 420, 520 and 600 °C to a damage level of 40 dpa (displacements per atom) with helium atoms implanted up to a concentration of 80 appm. Tensile tests showed that V–3Ti–1Si suffers the least amount of swelling, irradiation hardening and He-embrittlement. However, V–3Ti–1Si has the lowest thermal creep resistance among the three vanadium alloys.

Creep–rupture data at 650, 750 and 850 °C was used to develop a phenomenological stress rupture equation for the V–3Ti–1Si alloy. Among various creep–rupture data extrapolation techniques, the modified minimum-commitment-method (MMCM) [7] has the advantage of not being sensitive to creep data behavior. Results of the MMCM [8] analysis are depicted in fig. 1. Also shown are the TITAN-I first wall operating stresses during normal and off-normal operations. Allowable design stresses must include the effects of irradiation hardening and helium embrittlement. Limited helium embrittlement data [9] were used to estimate the allowable stresses after 1 full power year (FPY) of TITAN. This corresponds to an estimated damage dose of about 160 dpa. Our analysis indicates that the maximum allowable primary stress for V–3Ti–1Si is 108 MPa at 650 °C, 44 MPa at 750 °C, and 20 MPa at 850 °C.

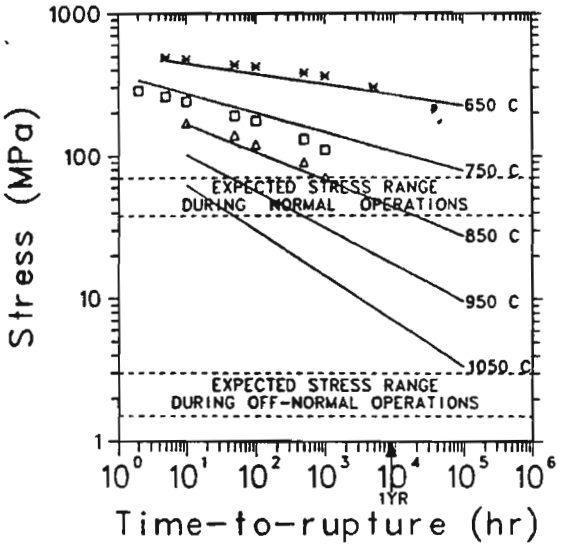

Fig. 1. Creep–rupture stress of V–3Ti–1Si at various temperatures (symbols are creep-rupture data points; solid lines represent MMCM calculations).

Coolant compatibility

One of the most significant advantages of vanadium alloys over ferritic alloys is their corrosion resistance to liquid lithium. At 600 °C the dissolution rate for vanadium is $\sim 5 \times 10^{-2}$ mg/m^2/h and for HT-9 about 50 mg/m^2/h [10]. Recently, a bimetallic loop experiment investigated the corrosion of V–3Ti–1Si in flowing liquid lithium [11]. The experiment consisted of high purity liquid lithium flowing at 7 cm/s in a titanium stabilized stainless steel (X10CrNiMoTi1810) loop at 823 K for a duration of up to 2056 h. The measured corrosion rate of V–3Ti–1Si was in the range of 10^{-2} to 10^{-3} g/m^2/h. The more significant finding, however, was the formation opf a very dense and adhesive vanadium-nitride layer ($(V,Ti)_xN$; $x \sim 1.56$–1.66). The thickness of the nitride layer (2–5 μm) was found to be exposure time independent. Another issue regarding coolant compatibility is the high lithium flow velocity (21 m/s at the TITAN-I first wall). Investigations showed that 21 m/s is far from the erosion threshold velocity of ~ 120 m/s, measured for most metals and ceramics [12]. Experiments [13] have been performed

with high velocity liquid lithium flowing at 50 m/s in Nb–1Zr tubes at 1073–1143°C. Measured corrosion rates after 500 h of lithium flow were about 0.1 mm/yr.

3. TITAN-II structural materials

TITAN-II is an aqueous loop-in-pool reactor design. For the water-cooled TITAN reactor, ferritic alloys are favored among structural material candidates. To reduce waste disposal management problems, low activation ferritic alloys are being developed. Preliminary evaluations indicate that a reduced activation alloy can be developed without compromising mechanical properties, primarily by replacing Mo by W. Several low activation ferritic alloys have been investigated. For the TITAN-II reactor the HEDL/UCLA 12Cr–0.3V–1W – 6.5Mn alloy (alloy 9-C) was chosen as structured material for TITAN-II primarily due to its good strength and elongation behavior after irradiation [14]. The high Cr content ensures excellent corrosion resistance and the low carbon content ensures better weldability characteristics, higher sensitization resistance, and reduced hydrogen embrittlement. The high concentration of Mn in alloy 9-C prevents the formation of delta-ferrite phases. The delta-ferrite phase formation is responsible for high DBTT and low hardness.

Alloy 9-C has a very high yield strength of 810 MPa and a high tensile strength of 1002 MPa at room temperature with a total elongation of 10.1%. Similar to other ferritic alloys, 9-C shows little or no irradiation hardening (change in yield stress) at low temperatures. At irradiation temperatures above 300°C alloy 9-C softens, having a total elongation of about 19% at 600°C after 14 dpa of damage dose. Table 1 shows selected irradiated and unirradiated properties of this alloy.

3.1. Aqueous solution compatibility

The tritium breeder in the TITAN-II reactor is a lithium salt dissolved in the water coolant. The salt chosen, based on the radiolytic behavior, is $LiNO_3$ (see next section). From a corrosion point of view the data base of corrosion of ferritics in $LiNO_3$ salt solutions is very limited. Indications are, however, that a high concentration of lithium nitrate aqueous salt solution does not exhibit unacceptable corrosion problems. Recent high temperature corrosion scoping experiments support this statement [15].

Stress-corrosion cracking (SCC) is a major concern in the nuclear industry. Most recent experiences with SCC in nuclear environments clearly show that SCC can be suppressed by reducing the oxygen content through the addition of hydrogen to the coolant [16]. The production of tritium in an aqueous lithium salt solution is therefore seen as an inherent SCC controlling mechanism. The proper choice of structural material can further reduce the probability of SCC. In particular a high Cr content coupled with a low C content are shown to reduce SCC. Both these requirements are fulfilled by alloy 9-C.

Table 1
Physical and mechanical properties of alloy 9-C (HEDL/UCLA) low-activation ferritic steel [14]

Property	Temperature (°C)					
	Unit	RT	300	400	500	600
Young's modulus	GPa	225	200	193	180	150
Poisson's ratio	–	0.4	0.4	0.4	0.4	0.4
Shear modulus [a]	GPa	83	75	72	68	–
Tensile strength	MPa	1002	–	810 [a]	942 [b]	749 [c]
Yield strength (irrad.) [c]	MPa	810	810	820	650	531
Total elongation (irrad.) [c]	%	10.1	13.8	15.0	17	19.4
Thermal exp. coeff.	10^{-6}/C	9.5	10.5	11	11.5	12
Specific heat	J/kg-°C	450	570	600	680	780
Electric resistivity	μΩ-m	0.6	0/82	0.9	0.99	1.05
Thermal conductivity	W/m-K	25	26.5	26.7	27.2	27.6
DBTT at 15/30 dpa [a]	°C	–	–	100/140	25/50	0/55

[a] Unavailable values replaced by HT-9.
[b] After 6 dpa of damage dose.
[c] Values given at irradiation temperatures after 14 dpa.

3.2. Radiolysis

Gamma-ray radiolysis yields of $LiNO_3$ salt solutions are known as a function of salt concentration [17]. At high concentrations the H_2 yields are very small and the H_2O_2 yield decreases by a factor of about 3 relative to pure water. Oxygen yields due to light particle radiation are fairly salt-concentration independent.

Alpha-ray radiolysis due to nuclear reactions with lithium in the aqueous $LiNO_3$ salt solution were estimated as a function of salt concentration based on the power law measurements of 3.4 MeV α's [18]. The oxygen production due to heavy particle radiation increases while the yields of H_2, H_2O, H, OH, and HO_2 all decrease with increasing salt concentration.

The limited data suggest that neither the light nor the heavy particle radiation of a highly concentrated $LiNO_3$ salt solution leads to high levels of radiolytic decomposition products, except for the formation of oxygen. In fact, an increase of salt concentration leads to a decrease in the production of H_2O_2, H_2, H, OH, and HO_2 and a slight increase in NO_2^- yields relative to highly diluted salt solutions [17].

The effect of elevated temperature on radiolysis was investigated. From experience gained in the fission industry with pure water [16], it can be ascertained that the stability of non-boiling water to radiolysis increases as temperature increases. The apparent stability is actually due to an increase in radical recombination reaction rates at elevated temperatures.

Although many uncertainties remain and much further research is required in the area of radiolysis, the use of a highly concentrated aqueous $LiNO_3$ salt solution should not lead to the formation of volatile or explosive gas mixtures. The effects of radiolytic decomposition products on corrosion, however, remain a subject of great uncertainty until a experimental data base of radiolytic decomposition products in a fusion environment becomes available.

4. Insulator material

The application of electrical insulators includes current breaks in various FPC components. Depending on their location, these breaks can be exposed to high radiation levels. Technical requirements for insulating materials include: adequate electrical resistivity, radiation stability, minimum radiation-induced conductivity, mechanical integrity, and fabricability.

Organic insulating materials generally do not meet high temperature requirements and also suffer from rapid resistivity degradation when exposed to ionizing radiation. Ceramic insulating materials, on the other hand, posses high melting or decomposition temperatures (> 2000 °C). Electrical conductivity (σ) values for various oxides and nitrides range from between 10^{-8} to 10^{-14} (ohm-cm)$^{-1}$ at 500 °C with BN having the lowest value. Exposed to a fusion reactor radiation field, ceramic insulators experience a change in their thermal conductivity, mechanical strength, electrical resistivity and in the dielectric breakdown strength (dbs).

A thermal conductivity independent of exposure time is favored because of higher confidence in the thermal behavior design of magnets and insulator-carrying components. The following insulators experience a 50–90% reduction in thermal conductivity after exposure to neutron irradiation: BeO, MgO, Al_2O_3, Y_2O_3, $Y_3Al_5O_{12}$, Si_3N_4, Si_2ON_2 and $Si_4Al_4O_2N_6$. Spinel ($MgAl_2O_4$) is one of the very few that does not show a reduction in thermal conductivity after neutron irradiation [19]. As far as tensile strength is concerned, $MgAl_2O_4$ shows an increase in strength upon irradiation [19]. Among the insulating materials, $MgAl_2O_4$ has shown good swelling resistance. In table 2 experimental swelling data are given [19]. A phenomenological swelling equation based on the swelling data of table 2 was developed [8]. Sample swelling calculations for spinel located at the OHF-coils of the TITAN-I reactor are demonstrated in fig. 2.

Based on the spinel swelling curves in fig. 2, a low or high operating temperature is favored. However, high temperatures degrade the dielectric breakdown strength (dbs) of ceramic insulators. The dbs is defined as the maximum potential gradient in the dielectric without the occurrence of electric breakdown. Below 200 °C the dbs for alumina is ~12 kV/mm. It drops to ~8 kV/mm at 350 °C and ~2.5 kV/mm at 700 °C. Thus, spinel offers good electrical resistivity even at high operating temperatures. Only components that need high resistivity values (> 12 kV/mm) have to operate at temperatures below 200 °C.

Table 2
Swelling of neutron irradiated spinel

Temp. (K)	$\Delta V/V$(%)	Fluence (n/cm^2) [a]
323	0.03±0.01	3.2×10^{22}
407	0.08±0.01	2.1×10^{26}
680	−0.19±0.01	2.2×10^{26}
815	−0.35±0.01	2.2×10^{26}
925	±0.01	2.3×10^{24}

[a] $E_n > 0.1$ MeV.

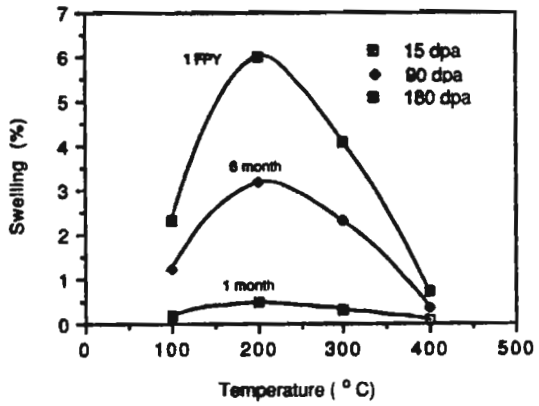

Fig. 2. Swelling of spinel as a function of exposure time and temperature located at the OHF and divertor coils.

Another process that leads to an increase in electrical conductivity is ionizing radiation (γ-rays). The γ-ray photons interact with electrons which results in an increase of conduction charge carrier concentrations. This phenomenon is a flux-dependent effect (instantaneous) commonly known as radiation-induced conductivity (RIC). RIC has been measured for alumina at temperatures below 300 °C and was found to be directly related to the ionizing dose rate (γ). Our analysis has shown that RIC for an 18 MW/m^2 neutron wall loading will increase the conductivity of spinel to about 3.5×10^{-5} $(\Omega m)^{-1}$. Al_2O_3 doping experiments using 0.03 wt.% Cr_2O_3 shows a reduction of conductivity by more than one order of magnitude. Similar doping techniques can be used to reduce the RIC of spinel.

5. Divertor-target material

The high particle fluxes encountered on impurity control components such as the divertor plates or the limiter, requires a high Z material to reduce the amount of sputtering. Simultaneously, high heat loads need to be dealt with and thus materials with high thermal conductivity and low thermal stresses are required. Among the refractory metals a tungsten–rhenium alloy has been selected. The workability and mechanical properties of W–Re alloys, with Re content in the range of 3–30 at.%, have been found to be excellent. Furthermore, the thermal expansion coefficient of W–Re alloys can be tailored to a degree by varying the Re content. Suitable brazing materials with different application temperatures have also been developed to join W–Re alloys with other alloys.

Of importance is the high ductile-to-brittle transition temperature (DBTT) below which it cannot be worked due to its extreme brittleness. Pure tungsten has a DBTT of about 200–400 °C depending on the impurity content, thermomechanical history, and thickness [20]. The addition of rhenium reduces the DBTT appreciably. Tungsten–26% rhenium has a DBTT of about 90 °C [20] which is a great improvement from the pure tungsten DBTT. The 90 °C DBTT requires that forming, cutting, milling, and drilling of this alloy must be done at temperatures well above this DBTT.

6. Summary

The following is a summary of findings of material selection issues for the liquid-lithium-cooled TITAN-I and the aqueous loop-in-pool TITAN-RFP compact fusion reactors: For the liquid-lithium-cooled TITAN-I reactor:

- V–3Ti–1Si was chosen over V–15Cr–5Ti due to its good radiation damage resistance, lower helium embrittlement, and lower swelling rates.
- From the limited available creep data it seems that V–3Ti–1Si is able to operate satisfactorily at elevated temperatures ($\leq$ 700 °C).
- Limited liquid lithium corrosion data indicate the possibility of a self-limiting corrosion rate on V–3Ti–1Si, due to the formation of a (V,Ti)-nitride surface layer.
- Such an in-situ layer formation can have "self-healing" properties.
- Low-swelling operating temperatures for spinel ($MgAl_2O_4$) have been identified. If operated outside 150–300 °C spinel shows excellent swelling resistance.
- The principal feasibility of using tungsten–rhenium alloys for the high heat flux components is no longer a major issue.

For the TTAN-II aqueous loop-in-pool design:

- A low activation ferritic alloy (alloy 9-C; HEDL/UCLA) has been identified as a viable structural material for fusion applications. It shows good strength and ductility behavior.
- Irradiation behavior data are sparse, but scoping experiments show good retention of mechanical properties.
- The high chromium and low carbon content of this alloy ensure good aqueous corrosion resistance and reduces the degree of hydrogen embrittlement, respectively.

- The choice of $LiNO_3$ over LiOH as a breeding salt dissolved in the coolant was based on the radiolytic behavior of the salt solutions.
- Radiolysis of $LiNO_3$ salt solutions was investigated in detail. Recent experiments with γ-rays clearly show a reduction of radiolytic decomposition of the water, except for oxygen. However, the produced tritium will readily combine with the oxygen.
- The use of $LiNO_3$ salt coupled with the production of tritium results in:
  - elevation of water boiling point
  - decrease of SCC of some ferrous alloys
  - reduction of hydrogen attack.
- Although the aqueous lithium-salt solution blanket concept shows promising features, detailed but relatively simple experimental investigations are needed before more decisive statements regarding the feasibility of a lithium salt aqueous solution blanket can be made.

Acknowledgement

Work supported in part by the United States Department of Energy under Contract DE-FG03-86ER52126.

References

[1] F. Najmabadi, R.W. Conn, N.M. Ghoniem et al., The TITAN reversed field-pinch fusion reactor study: Scoping phase report, Joint Report of UCLA, GA Technologies Inc., Los Alamos National Laboratory and Rensselaer Polytechnic Institute, UCLA-PPG-1100 (Jan. 1987).

[2] S.P. Grotz, N.M. Ghoniem et al., Overview of the TITAN-II fusion-power core, Fusion Engrg. Des. 8–10 (1989), in these Proceedings.

[3] C.P.C. Wong, R.L. Creedon, S.P. Grotz, E.T. Cheng, S. Sharafat, P.I.H. Cooke et al., Overview of the TITAN-II reversed-field pinch aqueous fusion power core-design, Fusion Engrg. Des. 8 (1989), in these Proceedings.

[4] F. Najmabadi, R.W. Conn, S.P. Grotz, N.M. Ghoniem, et al., The TITAN reversed field-pinch fusion reactor study: Final report, Joint Report of UCLA, GA Technologies Inc., Los Alamos National Laboratory and Rensselaer Polytechnic Institute, UCLA-PPG-1200 (March 1988).

[5] D.L. Smith, B.A. Loomis and D.R. Diercks Vanadium-base alloys for fusion reactor applications – a review, J. Nucl. Mat. 135 (1985) 125.

[6] D.N. Braski, The effect of neutron irradiation on the tensile properties and microstructure of several vanadium alloys, presented at the ASTM Conference on Fusion Reactor Materials, Seattle, Washington, June 1986.

[7] R.J. Amodeo and N.M. Ghoniem, Development of design equations for ferritic alloys in fusion reactors, Nucl. Engrg. Design/Fusion 2 (1985) 97.

[8] S. Sharafat, N.M. Ghoniem et al., Structure and insulator material choices for the TITAN reversed-field pinch reactor study, Proc. 12th Symposium on Fusion Engineering, Monterey, CA, October 1987, to appear.

[9] D.N. Braski, The effects of helium on the tensile properties of several vanadium alloys, ADIP Report DOE/ER-0045/13 (Sept. 1984).

[10] D.L. Smith, G.D. Morgan, M.A. Abdou, C.C. Baker, J.D. Gordon et al., Blanket Comparison and selection study, Final Report, ANL/FPP-84-1 vol. 2 (1984), p. 6.2–15.

[11] C.H. Adelhelm, H.U. Borgstedt and J. Konys, Corrosion of V–3Ti–1Si in flowing lithium, Fusion Technol. 8 (1985) 541.

[12] J.E. Field, S. van der Zwaag and D. Townsend, Liquid impact damage assessment for a range of infra-red materials, Proc. Sixth Int. Conf. on Erosion by Liquid and Solid Impact, Newnham College, UK, 3-6, Sept. 1983, pp. 21.1–21.13.

[13] E.E. Hoffman and R.W. Harrison, The compatibility of refractory metals with liquid metals, Proc. Symp. on Metallurgy and Technology of Refractory Metals, Washington, D.C., 25-26 April, 1968, pp. 251–287.

[14] D.S. Gelles, N.M. Ghoniem and R.W. Powell, Low activation ferritic alloys patent description, University of California, Los Angeles, Report, UCLA/ENG-87-9 PPG-1049 (1987).

[15] R. Waeben, W. Bogaert and M. Embrechts, Initial corrosion evaluation of candidate materials for an ASCB driver blanket For NET, Proc. 12th Symp. on Fusion Engineering, Monterey, CA, October 1987, to appear.

[16] P. Cohen, Water coolant technology of power reactors, American Nuclear Society (1980).

[17] M. Daniels, Radiolysis and photolysis of the aqueous nitrate system, in: Radiation Chemistry, Vol. 1, ed. R.F. Gould (Am. Chem. Soc., Washington D.C., 1968).

[18] M. Burton and K.C. Kurien, J. Phys. Chem. 63 (1959) 899.

[19] F.W. Clinard, Jr., G.F. Hurley, L.W. Hobbs, D.L. Rohr and R.A. Youngman, Structural performance of ceramics in a high-fluence environment, J. Nucl. Mat. 122&123 (1984) 1386.

[20] Metallwerk Plansee GmbH, Tungsten–rhenium alloys, in: Refractory Metals and Special Metals (PLANSEE, 1987).